

**IMPACT OF SKIRT PRESSING ON THE AERODYNAMIC DRAG OF
A BADMINTON SHUTTLECOCK.**

A DISSERTATION

SUBMITTED IN PARTIAL FULFILLMENT OF THE
REQUIREMENT FOR THE AWARD OF THE DEGREE
OF

**MASTER OF TECHNOLOGY
(THERMAL ENGINEERING)**

SUBMITTED BY

**GARVIT KUKREJA
ROLL NO. : 2K18/THE/05**

UNDER THE SUPERVISION OF

Prof. B.B. ARORA



DEPARTMENT OF MECHANICAL ENGINEERING

DELHI TECHNOLOGICAL UNIVERSITY

(Formerly Delhi College of Engineering)

Bawana Road, Delhi-110042

JUNE 2020

DEPARTMENT OF MECHANICAL ENGINEERING

DELHI TECHNOLOGICAL UNIVERSITY

(Formerly Delhi College of Engineering)

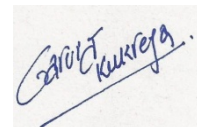
Bawana Road, Delhi-110042

CANDIDATE'S DECLARATION

I, **Garvit kukreja**, hereby certify that the work which is being presented in this thesis entitled **“Impact of skirt pressing on the aerodynamic drag of a badminton shuttlecock.”** is submitted in the partial fulfilment of the requirement for the degree of **Master of Technology (Thermal Engineering)** in Department of Mechanical Engineering at **Delhi Technological University** is an authentic record of my work carried out under the supervision of **Prof. B.B. Arora**. The matter presented in this thesis has not been submitted in any other University/Institute for the award of Master of Technology Degree. Also, it has not been directly copied from any source without giving its proper reference.

Place: Delhi

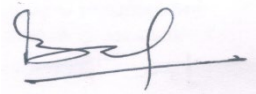
Date: 16/09/2020

A handwritten signature in blue ink that reads "Garvit kukreja" with a horizontal line underneath.

Garvit kukreja
(2K18/THE/05)

CERTIFICATE

This is to certify that this thesis report entitled, “**Impact of skirt Pressing on the Aerodynamic Drag of a Badminton shuttlecock.**” being submitted by **Garvit kukreja (Roll No.: 2K18/THE/05)** at Delhi Technological University, Delhi for the award of the Degree of Master of Technology as per the academic curriculum. It is a record of bonafide research work carried out by the student under my supervision and guidance, towards partial fulfilment of the requirement for the award of Master of Technology degree in Thermal Engineering. The work is original as it has not been submitted earlier in part or full for any purpose before.



Prof. B.B. Arora
Professor
Mechanical Engineering Department
Delhi Technological University
Delhi-110042

ACKNOWLEDGEMENT

First and foremost, praises and thanks to God, the Almighty, for His showers of blessings throughout my research work to complete the research successfully.

I would like to extend my gratitude to **Dr Vipin**, Head of Department of Mechanical Engineering, Delhi Technological University, for providing this opportunity to carry out the present thesis work.

I would like to express my deep and sincere gratitude to my research supervisor, **Prof. B.B. Arora**, Department of Mechanical Engineering, Delhi Technological University, for allowing me to do research and providing invaluable guidance throughout this research. His dynamism, vision, sincerity and motivation have deeply inspired me. He has taught me the methodology to carry out the research and to present the research works as clearly as possible. It was a great privilege and honour to work and study under his guidance. I am extremely grateful for what he has offered me. I would also like to thank him for his friendship, empathy, and a great sense of humour. Without the wise advice and able guidance, it would have been impossible to complete the thesis in this manner.

I am extremely grateful to my parents and family for their love, prayers, caring and sacrifices for educating and preparing me for my future.

GARVIT KUKREJA
2K18/THE/05
M.TECH
THERMAL ENGINEERING

ABSTRACT

The effects of the various design parameters of the shuttlecock have been attempted to design a synthetic shuttlecock having a similar feature that of feather shuttlecock. Most of the work till date has been attempted to visualize the flow behavior around the shuttlecock. Work has been done to obtain the shuttlecock flight trajectory. A little work has been done on changing the design parameter of the shuttlecock. The impact of skirt pressing on shuttlecock has not been studied in detail until now. Reynolds-Averaged Navier strokes (RANS) model was applied to evaluate the performance parameters of the shuttlecock. It has been observed from the study that the addition of radial or axial pressing over skirt decreases drag coefficient, contrary to which when both pressings added together Drag Coefficient increases. Another effect which was studied was the effect of increasing the pressing length overskirt which results in increasing the drag coefficient.

TABLE OF CONTENTS

CANDITATE’S DECLARATION	i
CERTIFICATE	ii
ACKNOWLEDGEMENT	iii
ABSTRACT	iv
TABLE OF CONTENT	v
LIST OF FIGURE	vii
LIST OF TABLES	ix
LIST OF SYMBOLS	x
CHAPTER 1: INTRODUCTION	1-3
1.1 BACKGROUND	1
1.2 MOTIVATION	2
1.3 OBJECTIVE	3
1.4 SCOPE	3
CHAPTER 2: LITERATURE REVIEW	3-16
2.1 BADMINTON SHUTTLECOCK	3
2.1.1 FEATHERED SHUTTLECOCK	3
2.1.2 NON-EATHERED SHUTTLECOCK	4
2.2 FLOW ALONG SHUTTLECOCK	5
2.3 AERODAMICS EXPERIMENTS ON SHUTTLECOCK	11
2.3.1 FLIGHT EXPERIMENT O SHUTTLECOCK	11
2.3.2 SPIN EXPERIMENT	15
2.4 SUMMARY	16
CHAPTER 3: AERODYNAMICS OF SHUTTLE	17-24
3.1 MODEL GEOMETRY AND ANSYS FLUENT METHOD	18
3.2 NOMENCLATURE OF SHUTTLE	20
3.3 MESH AND BOUNDARY CONDITION	21
3.4 SOLUTION METHOD	21
3.5 VALIDATION	22
3.6 GRID-INDENDENT TEST	23

CHAPTER 4: RESULTS AND DISCUSSIONS	25-30
4.1 FLOW OVER A PERECT GAPLESS CONICAL SKIRT	25
4.2 DRAG COEFICIENT	26
CHAPTER 5: CONCLUSIONS AND FUTURE SCOPE	31
5.1 CONCLUSIONS	31
5.2 FUTURE SCOPE	31
REFERENCES	32

LIST OF FIGURES

CHAPTER 1: INTRODUCTION

Figure 1: Description of shuttlecock, as given by cooke

CHAPTER 2: A literature review

Figure 2: Show a hollow cone shuttlecock without holes on skirt, used as a fundamental base model.

Figure 3: Smoke Flow over feather & synthetic shuttlecock

Figure 4: Shows a flow in the wake zone of a shuttlecock

Figure 5: Modified shuttlecock with a lower skirt covered [7].

Figure 6: Modified synthetic shuttlecock with upper, lower, complete skirt covered [7].

Figure 7: Variation of drag coefficient with Reynolds number for various models of shuttlecock [2].

Figure 8: Graphical description of the conical model with a gap.

Figure 9: Variation of Drag forces with surface area [6].

Figure 10: Illustration of a pre-stall and post-stall regime of steady-state flight [4].

Figure 11: Different types of shuttle o which Cooke [9] performed experiment.

Figure 12: Predicted vs. Measured trajectory data for all shuttlecocks [9].

Figure 13: Coordinate of 2D force system of the shuttlecock [9].

Figure 14: Illustration of shuttlecock heading concerning flight path

in the unsteady state flight [].

CHAPTER 3: AERODYNAMICS OF SHUTTLECOCK

Figure 15: Classification of shuttlecocks.

Figure 16: Different types of shuttlecock, a: gapless shuttlecock without Axial and Radial Pressing

Figure 17: Different type of pressing length used in the models. Model X has no pressing while other models show pressing from 10mm to 60mm in an interval of 10mm.

Figure 18: Show Shuttlecock NN4A, Which is having 4mm Axial pressing only, D Shows radial pressing due to Axial pressing.

Figure 19: Mesh around shuttlecock.

Figure 20: Shuttle within cylindrical fluid domain

Figure 21: shows the Coefficient of pressure result x-axis shows the length of the shuttlecock in and y-axis Shows Pressure coefficient.

CHAPTER 4 : RESULT & DISCUSSION

Figure 22: Velocity vector around a gapless shuttlecock.

Figure 23: Variation of drag coefficient of various models with different pressing length.

Figure 24: Variation of Skirt Surface area with Pressing length.

Figure 25: Drag coefficient & Frontal area Vs. Shuttlecock.

Figure 26: Pressure contours on the top portion of the shuttlecock skirt.

Figure 27: Pressure vs radial distance from the centre of the shuttlecock on the top portion of the shuttlecock.

Figure 28: Drag Coefficient Vs. Skirt pressing with Different Models.

LIST OF TABLES

Table 1: Types of shuttlecocks.	5
Table 2: Dimension and areas of gaps for the various models [4].	10
Table 3: Skirt Surface area and frontal area of shuttlecocks.	18
Table 4: Example of Nomenclature of shuttlecock, 6RNN2.	20
Table 5: Example of Nomenclature of shuttlecock, 4R4A2.	20
Table 6: Example of Nomenclature of shuttlecock, NN4AN.	20
Table 7: Difference in Drag coefficient from the course and Fine mesh. Elements are in millions.	24
Table 8: Difference in drag on 10mm ad 60mm skirt pressing length.	20

LIST OF SYMBOLS

m	mass of shuttlecock,
D	Drag force
L	Lift Force
θ	angle between velocity vector and horizontal datum
β	angle between velocity vector and horizontal datum – the pitch angle
g	acceleration due to gravity
M	aerodynamic pitching moment
α	angle of attack
x	horizontal distance, \ddot{x} and \ddot{y} are the acceleration in the horizontal and vertical direction
y	height
v_t	terminal velocity
v_t'	the first time derivative of terminal velocity
v_{yi}	initial velocity in Y-direction.
$.v_{xi}$	initial velocity in the X-direction

1. Introduction

1.1 Background

Today's, badminton game is originated from 'Shuttle and battledore' in the 1860s. In which players have to bat the shuttlecock from one to the other as many times as possible without allowing it to fall to the ground.

Badminton: A racket sport which is played by two opposing player or pair of opposing players who stand in the opposite halves of the rectangular court which is divided by a net. The game is to hit the shuttlecock once with the badminton and so that it passes over the net and lands in the opponent court. The shuttlecock should cross the net by only one hit by each team and the rally ends when the shuttlecock struck the ground.

The game is governed by the 'Badminton World Federation' which was established in 1934 in England. Its initial name was 'International Badminton Federation'. which was later changed to BWF in 2006 and, its headquarter shifted to Malaysia in 2005.

Shuttlecock has a unique aerodynamic property which causes it to fly differently than balls which are used in most of the other racket sports. Shuttlecock usually flies at a much higher speed when compared to balls of other racket sports and have a world record of 332km/h set in Sudirman cup in Beijing in the year 2005. Interestingly even reaching so much speed when shuttlecock reaches the opponent end its usually on very low speed and its credit goes to its feather in case of feather shuttlecock and skirt in case of the synthetic shuttlecock which is a high drag-inducing part and decelerates the shuttlecock at a very high rate.

In the year 1952, with the innovation of injection moulded synthetic shuttlecock the game earned a lot of broader appeal. Soon after with the debut of the game in Barcelona Olympics in the year 1992 the game eared the much more recognition.

. The sport demands excellent fitness: players require aerobic stamina, agility, strength, speed, and precision. It is also a technical sport, requiring good motor coordination and the development of sophisticated racket movements.

Badminton, the world's second most loved game, which is played by around 220million people around the world regularly.

However, the major problem that comes with the popularity of badminton is the dearth of a good quality feather which can be used for the manufacturing of badminton shuttlecock. The reason for this is that the supply of feather is dependent on several peripheral aspects. This implies that manufacturers are more attracted to the development of synthetic shuttlecock instead of feather shuttlecocks. However, players still prefer feather shuttlecock as they believe synthetic shuttlecock behaves differently from the feather shuttlecocks because they are used to the shuttlecock flight behaviour and expect the flight trajectory.

1.2 Motivation

The literature reviewed indicates that it is not possible to fully understand and evaluate the features of the shuttle through these works. Plenty of work that can be done to completely understand the badminton shuttlecocks, and can contribute to ease of development and testing a new shuttlecock. It is considered that comparing the numerous types of shuttlecocks under same conditions will improve our understanding in this field. Moreover, consistency in result and sensitivity to variation can be ensured by a well-defined test methodology while assessing a reference shuttlecock against the other shuttlecock.

1.3 Objectives

The purpose is to design a synthetic shuttle which behaves alike feather shuttlecock because of the limitation with which feather shuttlecock comes, those are

- Even if one of the feathers comes out of the cork its of no use.
- Production depends on external factors like government policy and Health of Goose of which feather is being used.
- Large production is again a challenge.

The synthetic shuttlecock fulfils all of the above drawbacks, it uses synthetic polyMer which maintains its durability and manufactured on Injection moulding due to which large production is possible.

1.4 Scope

The extent of this study is as follows:

To study the impact of skirt pressing of the badminton shuttlecock through flow simulation around the shuttle. As the skirt changes the pressure difference around the shuttlecock get changes and drag on the shuttlecock changes which affect the flight of the shuttlecock. Therefore Pressing acts as the drag-inducing feature and its effect should be studied to understand the flight performance of the shuttlecock. Pressing is shown in figure (1) as stated by cooke[1].

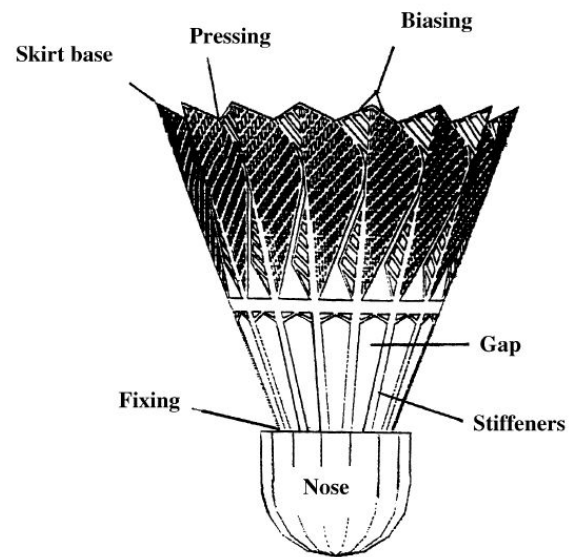


Figure 3: Description of shuttlecock, as given by cooke [1].

2. Literature review

2.1 Badminton Shuttlecock

A shuttlecock for badminton has two sections: one is cork which is a combination of hemispherical dome and a cylinder, dome being in front cylinder. Another is a skirt which can be of feathers or synthetic polymer.

For the approval of shuttlecock from Badminton world federation(BWF), there are only one testing criteria for all the type of shuttlecock which is its flight characteristics should be similar to those which are produced by feather shuttlecock whose cork is covered by a layer of thin leather.

2.1.1 Feathered Shuttle

1. The shuttlecock should have 16 feathers which are fix in the base.
2. The feather should be of the uniform length of 62mm to 70mm from the tip of the skirt to the base in the cork.
3. The diameter of the tip of the skirt should be of 58mm to 68mm.

4. Thread or any other suitable material can be used for firmly fastening the feathers.
5. The cork of the shuttlecock should be of a diameter of 25 mm to 28mm with a hemispherical dome at the bottom of the cylindrical portion.
6. The weight of shuttlecock should be in the range of 4.74 to 5.50 grams.

2.1.2 Non-Feathered Shuttle

1. The skirt material should replace natural feathers.
2. The weight should be in range as of the feather shuttlecock. Skirt and base dimension should also be in range as described for feather shuttlecock. However, because of the difference in the specific gravity and other properties of synthetic materials in comparison with feathers, a variation of up to 10 per cent shall be acceptable.

The large dimensional tolerance is available for the shuttlecock design. Which provide diverse flight behaviour to shuttlecock ee when it is designed as per standards. These large dimensional tolerances are given in accordance to make shuttlecock of same flight characteristics in different atmospheric condition. It implies that two distinct shuttles, which are having very diverse flight performance, both are allowed for use.

Shuttlecocks which used for tournaments are only required to get approved from Badminton World Federation, other shuttles which are used for non-tournament use don't need approval from BWF. As affirmed by C.S.H. Lin [4], Mizuno Launched the NS-300 shuttlecock in the year 2009 which was made-up of 15 synthetic feathers in the similar assortment as of the traditional feather shuttle which is having 16 feathers. This shuttlecock didn't get the approval from the BWF. But, it didn't have an effect on the acceptance of the NS-300 as it was meant to be used for the non-tournament purpose only.

A variety of shuttles are offered in the marketplace. They come in a variety of option like traditional natural feather ones and others with sophisticated artificial feathers. Shuttlecocks manufactured with different masses so that player can play with proffered speed. Various shuttles can be described as follows:

Table 3 Types of shuttlecocks

Shuttle Color	Mass	Speed	Center of mass
Red	High	High	Closer to the nose.
Blue	Intermediate	Intermediate	Intermediate
Green	Low	Low	Away from Nose.

2.2 Flow along with shuttlecock

Features along the conical skirt are used for inducing Drag in shuttlecock. Fundamentally a shuttle can be represented by a combination of a cork and a gapless cone. Cooke [1], Kitta et al. [3], Verma et al. [2] and CSH Lin [4] used this approach. Cooke [1] investigated the flow around a gapless shuttlecock through experiments, a gapless shuttlecock is shown in Figure 2.

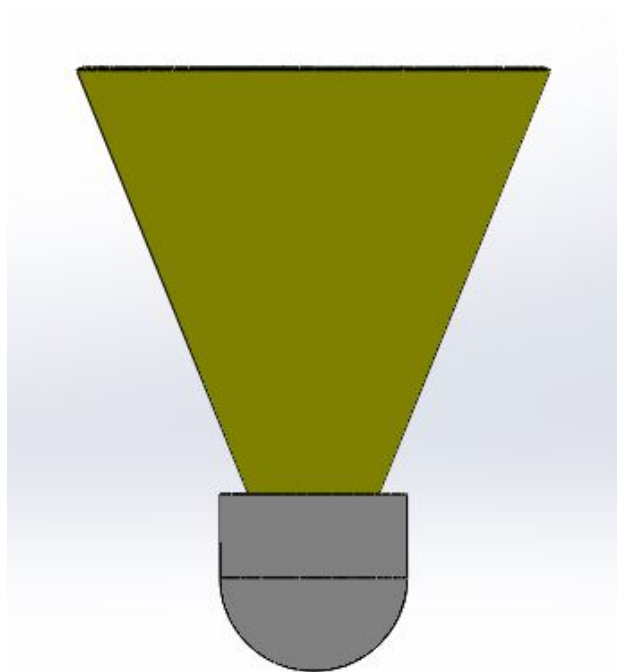


Figure 4: Show a hollow cone shuttlecock without holes on the skirt, used by Cooke [1], Kitta et al. [3], Verma et al. [2] and CSH Lin [4], used as a fundamental base model.

Cooke [1] Flow visualization revealed that the shuttlecock is a bluff body and predominant drag mechanism is a base drag, The flow separates at the downstream end of the nose and reattaches on the skirt, as shown in figure 3, smoke flow visualization techniques are used at Re. No. 4400, which shows that there is a stagnation area behind the solid part of the skirts of both feather and synthetic skirt type shuttlecocks and feather shuttlecocks figure 3(a) provide more complete blockage. The gaps in skirt results in air bleeding which decreases the air pressure on the inner surface of the skirt and creates a jet of air in the wake. The jet of air through the feather shuttlecock merges with the outer flow and creates an unsteady, irregular wake pattern which curls inwards.

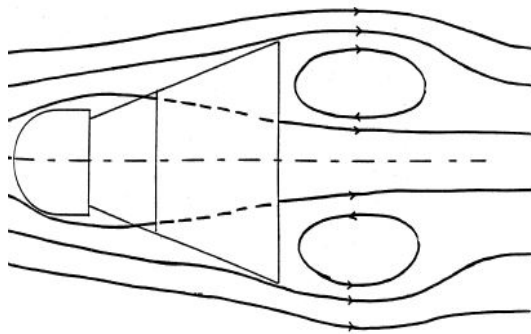
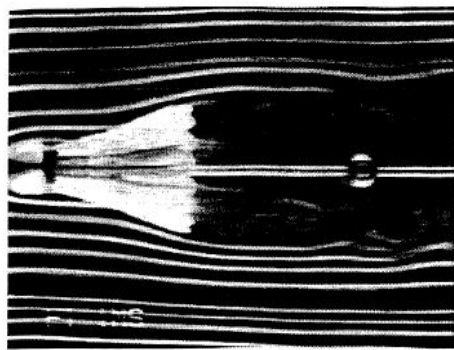


Figure 3 (a)

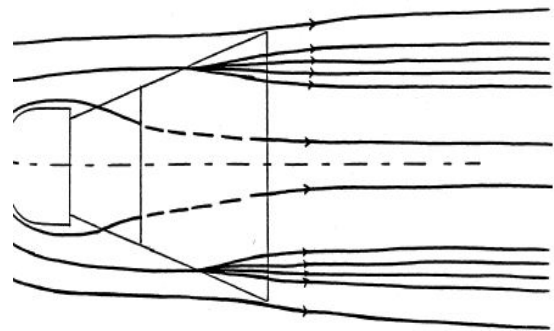
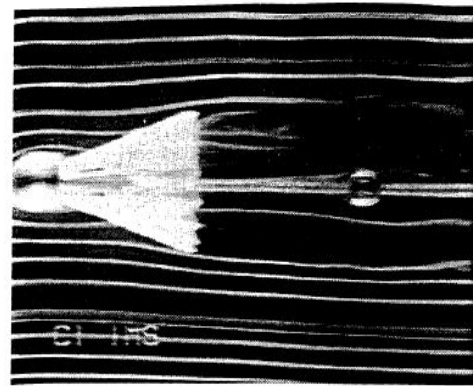


Figure 3 (b)

Figure 5: Figure 3. 3(a): Smoke Flow over feather shuttlecock, 3(b) Smoke Flow over synthetic shuttlecock at Re.=4400 [1].

It is a generally described characteristics of blunt body flow. Unlike the synthetic shuttlecock, the feather shuttlecock has little or no skirt porosity. It is observed that introducing gaps into the skirt increases drag.

Cooke [1] did an experimental study on the feather and a synthetic shuttlecock to which she concluded that both the of shuttlecock have almost same drag coefficient at lower speed and

drag decreases for synthetic shuttlecock at a higher speed because of decrease in the frontal area of the synthetic shuttle which remains same for feather shuttlecock.

Calvert [6], conducted a comparative study between a solid cone without a cork and shuttlecock with holes in which he dogged that the flow regime doesn't change upstream of the cork in a different model of shuttlecocks. Further, he proposed that hole on the skirt increase the air bleeding which increases drag coefficient. Kitta et al. [3] further investigate the flow around a gapless shuttlecock model.

Kitta et al. [3] examined the flow around a gapless hollow cone shuttle. This hollow cone shuttle was modelled by closing the gaps of the feather shuttlecock by applying cellophane tape. When experimental comparison made with shuttlecock with gaps, it was observed that drag reduces when the gaps were capped. Flow visualization revealed that when gaps were open the jets of air passes through gap and reduces air pressure on the inner surface of the skirt. which increases the pressure difference thereby increasing the drag as proposed by Cooke[1]. Kitta et al. [3] also concluded that the drag coefficient remains almost constant over the range of Reynolds number when the shuttlecock is rotating about its axis. He experimentally showed that the in case of gapless shuttlecock all the flow passes over the skirt which makes flows at a faster speed in comparison to ordinary shuttlecock with a hole in which some of the flow passes through holes and which forms a rolled-up vortex in the wake region. As shown in figure

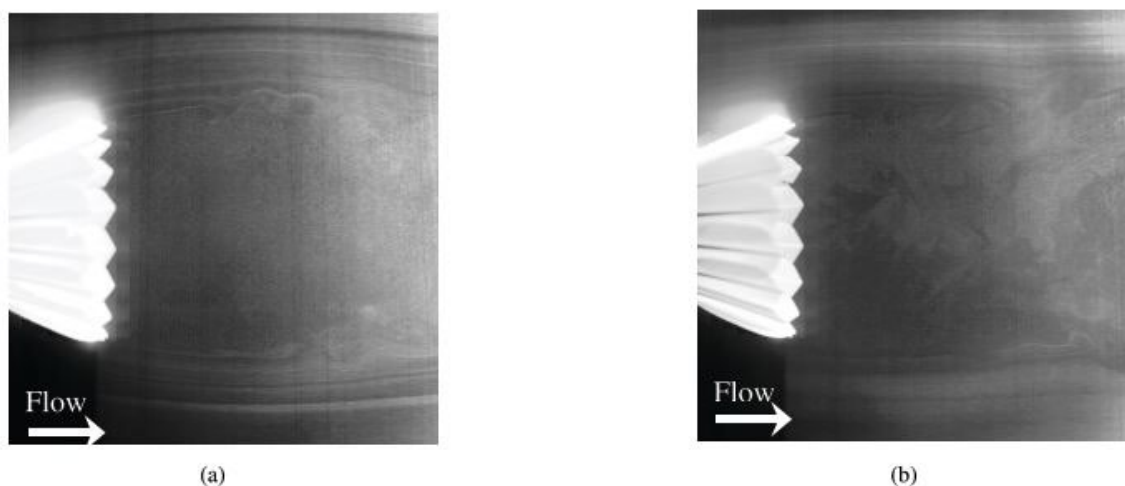


Figure 6: Shows a flow in the wake zone of a shuttlecock. (a) shows solid skirt shuttlecock, (b) shows feather shuttlecock[3].

A similar experimental investigation is done by Firoz Alam[7] in which Feather shuttlecocks were modified by closing the gaps in a lower skirt, and synthetic shuttlecock was modified in 3 ways that are, by closing the base gaps, skirt gaps, and the whole skirt section as shown in figures(5),(6). It was found through experiments that feather shuttlecocks with gaps closed possess drag coefficient equal to that of a corresponding cone. Fully covered synthetic shuttlecock has a drag coefficient value slightly higher than the shuttlecock with a lower skirt covered. He also studied the drag coefficient of 10 different types of synthetic and feather shuttlecock at a speed of 100km/hr. To which he concluded the average drag coefficient as 0.61, the lower value of the drag coefficient is because of skirt deformation at a higher speed.



Figure 5 : Modified shuttlecock with lower skirt covered [7].



Figure 6: Modified synthetic shuttlecock with upper, lower, complete skirt covered [7].

Verma et al [2] did a comparison between gapless shuttlecock, a feather shuttlecock and a synthetic shuttlecock and similar observations were made as of cooke[1], Kita[3], firoz[7]. The drag coefficient of the gapless cone skirt was lower than the feather and synthetic shuttlecock. Results of which are shown in figure [7]

Verma et al [2] also concluded that feather shuttlecock have much stronger axial jets and fluid near feathers acquire large tangential speed which leads to streamwise vorticity while in case of synthetic shuttlecock holes over skirt helps the fluid to move outside at the upper end of the skirt due to which its tangential speed is significantly smaller, but fortunately skirt stiffness in synthetic shuttlecock helps in attaining streamwise vorticity. He also studied the portion-wise drag contribution and concluded that feather region in case of feather shuttlecock and net in case of synthetic shuttlecock contribute the maximum drag.

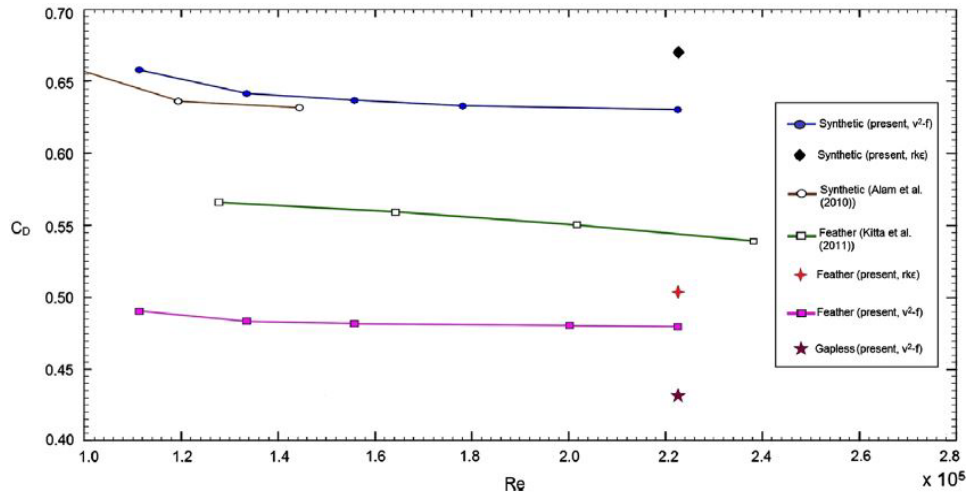


Figure 7: Variation of drag coefficient with Reynolds number for various models of shuttlecock [2].

Effect of twist angle of feathers is studied by Verma et al [2] only, as the angle is increased the gaps between feather increases which lead to the strong axial jet formation. Drag first increases with increase in the twist and then after it decreases after the critical angle which is 12 degree.

John[8] did a comparative study between RANS and Scale resolving simulation (SRS) for predicting the flow field of Synthetic shuttlecock, it was found, that unsteady RANS was capable of predicting the time average flow field which is comparable to SRS model and RANS was incapable of predicting turbulent vortex which is present in shuttle wake. However, both models predicted feasible Drag coefficient.

The effect of the gaps on the lower portion of shuttlecock skirt on the flow field and variation in flow variables i.e. pressure, velocity, Drag coefficient and pressure coefficient are studied by CSH Lin[4]. He considered six different profiles with different gaps, as shown in figure (8) and dimensions of different shuttlecocks are given in table (4).

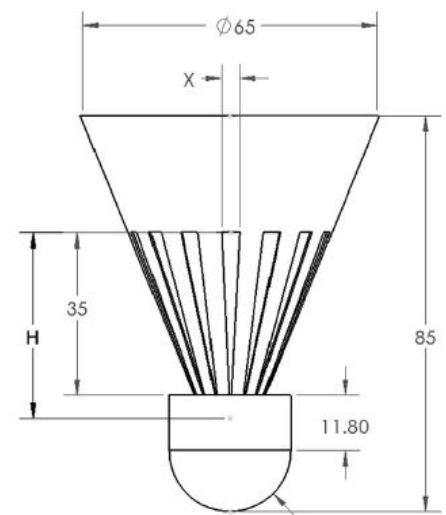


Figure 8: Graphical description of the conical model with gap. All dimensions are in mm.

Table 4: Dimension and areas of gaps for the various models [4].

Profile	Width (X/mm)	Height (H/mm)	Surface (area/mm ²)	Surface area Reduction (%)
A	N.A	N.A	8420	0
B	2	20	7865	6.59
C	2	40	7551	10.32
D	4	40	6910	17.93
E	6	40	6268	25.56
F	7.5	40	5784	31.31

He concluded that a shuttlecock having a hole on the lower portion of its skirt have up to 42.5% of more drag force when compared to the gapless shuttlecock. The drag force increases as the gap size are increased up to the critical size of the hole and beyond that gap size darg force again decreases. This also shows the blunt-body effect of the shuttlecock. Change of drag force with a decrease in surface area is shown in figure(9).

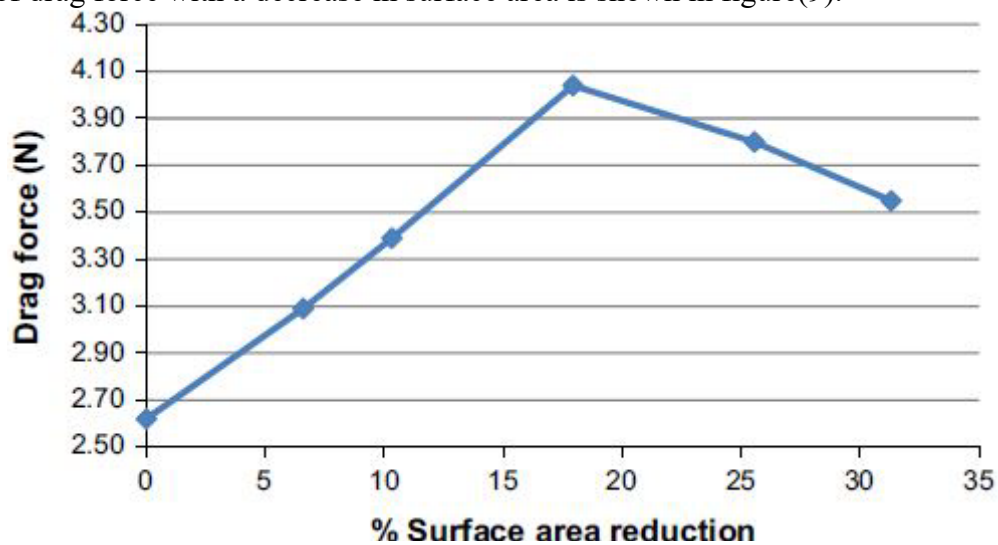


Figure 9: Variation of Drag forces with surface area [6].

When pressure profile is analysed it is observed that differential pressure increases between the outer and the inner surface of the skirt as the gap size increased which produces more drag. There is a formation of air jets due to the flow of air through the hole in the lower portion of the skirt. These air-jet reduces the recirculation of air in the wake of the shuttlecock.

2.3 Aerodynamic Experiments on Shuttlecocks

2.3.1 Flight Experiments on Shuttlecocks

Flight trajectory is the performance indicator of a shuttlecock. Feather shuttlecocks and synthetic versions have significantly different flight trajectory. Since players are familiar with feather shuttlecock, consider the synthetic shuttlecock as mediocre and unpredictable. According to Foong and Tan [5], the “ideal” flight trajectory is obtained from the ordinary

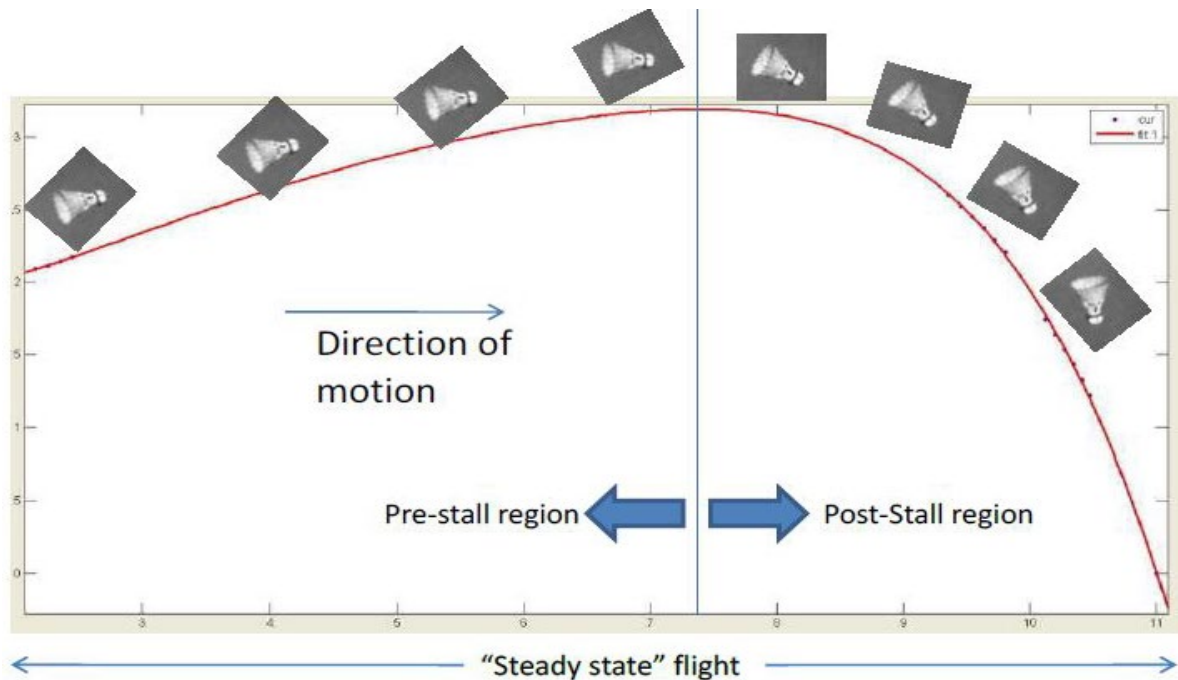


Figure 10: Pre-stall and post-stall regime of steady state flight [4].

feather Shuttlecock has a trajectory which is much distinctive from an ideal projectile motion. If a shuttlecock launched at a velocity which is lower than its terminal velocity then it will follow a parabola path which is ideal projectile motion. But when it is launched at a velocity more than its critical velocity then it will follow a trajectory which resembles the cannonball curve, in which descent path is more like perpendicular drop which is in contrast to the initial ascent which follows a parabola curve, as illustrated by CSH Lin[4] in figure (10).

Shuttlecock flight is categorized by four types- Smash, Clear, Net and Serve. The launch velocity of the net shot is less than the terminal velocity and shuttles follow a parabola curve, whereas in the remaining three shots shuttle velocity is more than the terminal velocity and shuttlecock follow a Tartaglia flight curve.

In 2002, Cooke[9] conducted a simulation for the trajectory of a badminton shuttlecock and considered the design parameters which will affect the 2-D motion of shuttlecock, i.e: mass,

area, drag, lift and pitching moment coefficients, a moment of inertia and damping factor. The research confirmed the difference in the trajectory of feather and synthetic shuttlecock during different shots. High clear, smash, low serve, net shot were modelled and analyzed using four different shuttlecocks as shown in figure(11). Procork, tournament, championship shuttlecock are made up of synthetic material, while the last one is feather shuttlecock.

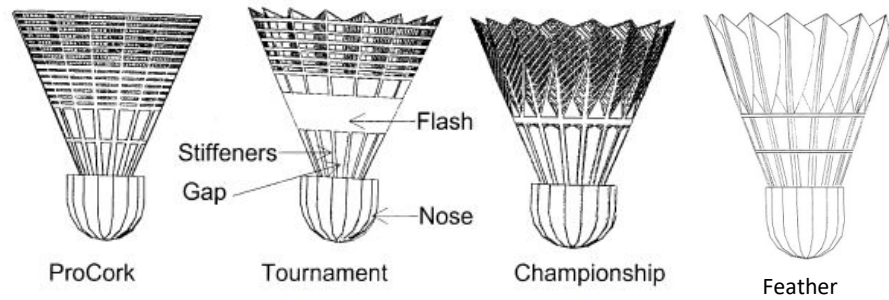


Figure 11: Different types of shuttlecock which Cooke [9] performed experiment.

In research, feather shuttlecocks were launched by using compressed air from a custom-produced air compressor. A comparison is made between the observed trajectory and the simulated trajectory. The simulated and observed trajectory from experiment found to be agreed within 5%. Predicted and measured trajectory data for different shuttlecocks are shown in figure 10(a) and for different shots in figure 10(b).

The equations of motions[9] which were used for predicting the quasi-steady state motion of the shuttlecock throughout its trajectory is given below.

$$m\ddot{x} + D \cos \theta + L \sin \theta = 0 \quad \text{Equation 1}$$

$$m\ddot{y} + D \cos \theta + L \sin \theta + mg = 0 \quad \text{Equation 2}$$

$$I_t \ddot{\beta} + c\dot{\beta} + \left| \frac{dM}{dx} \right| \alpha = 0 \quad \text{Equation 3}$$

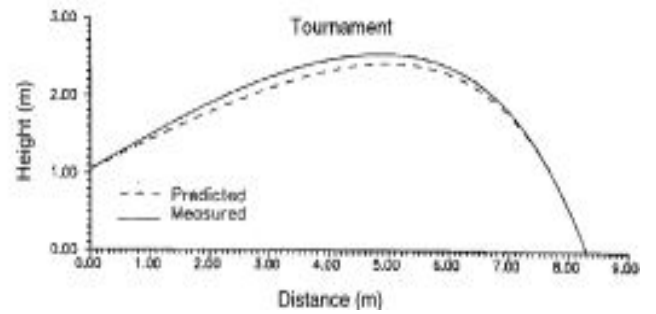
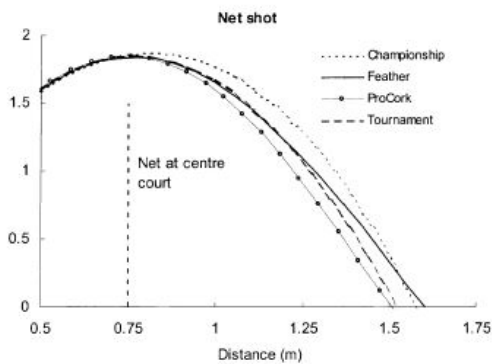
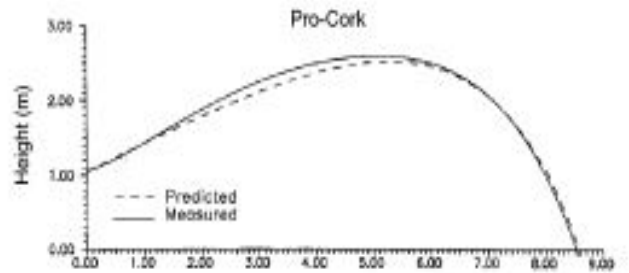
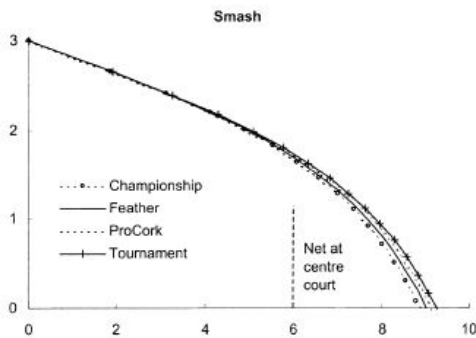
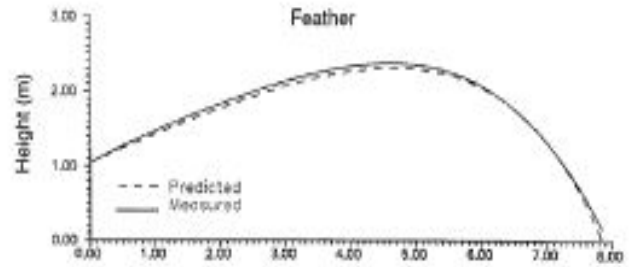
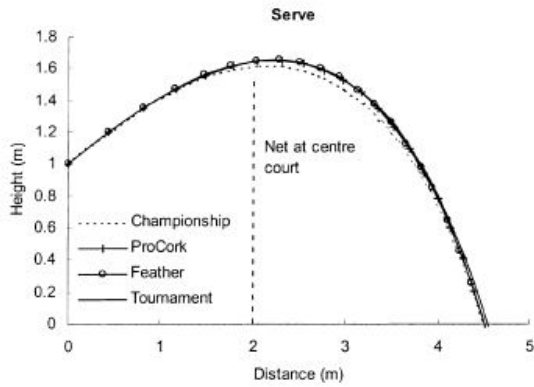
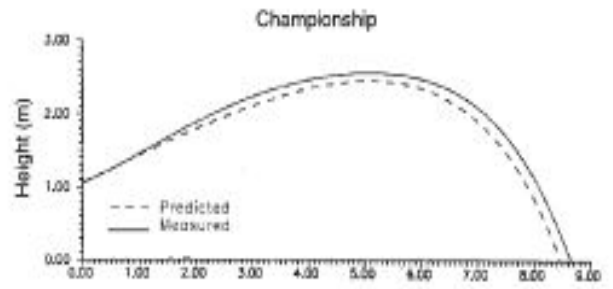
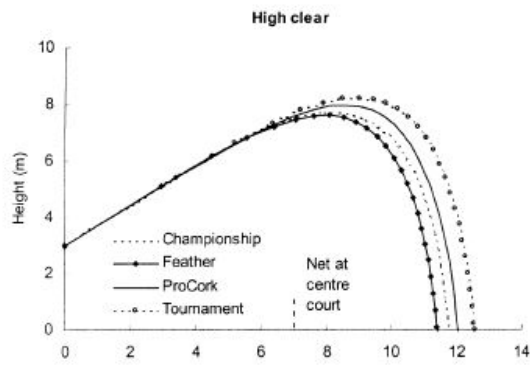


Figure 12(a)

Figure 12(b)

Figure 10: Predicted vs. Measured trajectory data for all shuttlecocks [9]. 12(a) shows Different shot, 12(b) Shows different shuttlecock results.

Where m is mass of shuttlecock, D is drag force and L is the lift force, θ is the angle between the velocity vector and horizontal datum, β is the angle between the shuttlecock axis and the horizontal datum-the pitch angle, g is the acceleration due to gravity, M is aerodynamic pitching moment, α is the angle of attack, x horizontal distance, \ddot{x} is acceleration in horizontal direction and \ddot{y} is the acceleration in the vertical direction, details are given in figure (13).

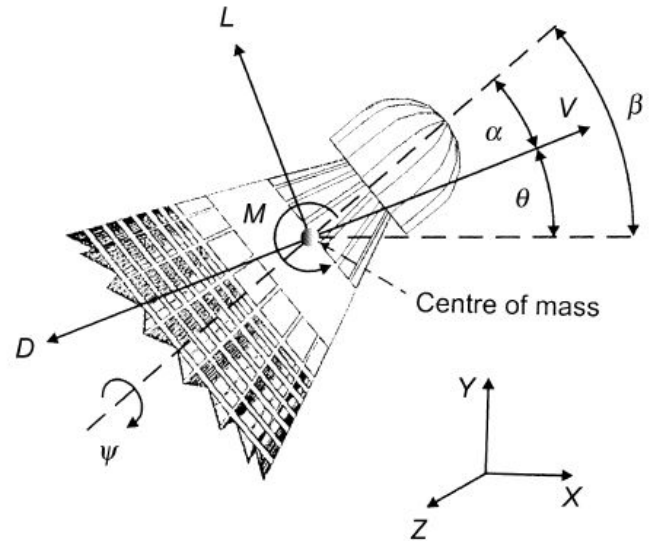


Figure 13: Coordinate of 2D force system of the shuttlecock [9].

The second approach uses a mathematical-based model for determining the trajectory of the shuttlecock. This is the approach is taken by Chen et al. [10] in his research. The used equation is given below.

$$y = \frac{v_t'^2}{g} \ln \left| \frac{\sin \left[\frac{v_t'}{v_{xt}} \left(e^{\frac{gx}{v_t'^2}} - 1 \right) + \tan^{-1} \left(\frac{v_t'}{v_{yt}} \right) \right]}{\sin \left[\tan^{-1} \left(\frac{v_t'}{v_{yt}} \right) \right]} \right| \quad \text{Equation 3}$$

Where y is the height of the shuttlecock, v_t refers to terminal velocity, v_t' is the acceleration of the terminal velocity, v_{xt} and v_{yt} are the initial velocities in x and y direction respectively. By applying numerous initial boundary conditions to the equation, we will able to simulate the trajectory of different shuttlecocks.

Surprisingly, BWF doesn't perform any of these experiments for determining the trajectory of a shuttlecock and nor have any regulation for inspection of shuttlecock trajectory. Rather, BWF performs only a speed test, which is given below, as stated by BWF in section 3ad of the rulebook.

1. To test a shuttlecock, a player shall use a full underhand stroke which makes contact with the shuttle over the back boundary line. The shuttle shall be hit at an upward angle and in a direction parallel to the sidelines.
2. A shuttle of correct speed will descend not less than 530 mm and not more than 990 mm short of the other back boundary line.

2.3.2 Spin Experiments

So far, most of the work has been done on measurement quasi-steady axial spin rate of the shuttlecock in the wind tunnel.

Quasi-steady state is achieved when the shuttlecock leaves the racket and turns over & takes up the constant shape and experiences linear deceleration, spin, pitching and yaw as explained by CSH Lin[4] as shown in figure(14). No experiment has been performed for the actual axial spin rate of the in-flight shuttlecock. The reason for this is that the acceleration and deceleration of spin occur in very less time. Further, due to high drag shuttlecock experiences an enormous change in linear speed during flight, which makes it almost impossible for a shuttlecock to attain steady-state spin in actual in-flight condition. a shuttlecock to attain steady-state spin in actual in-flight condition.

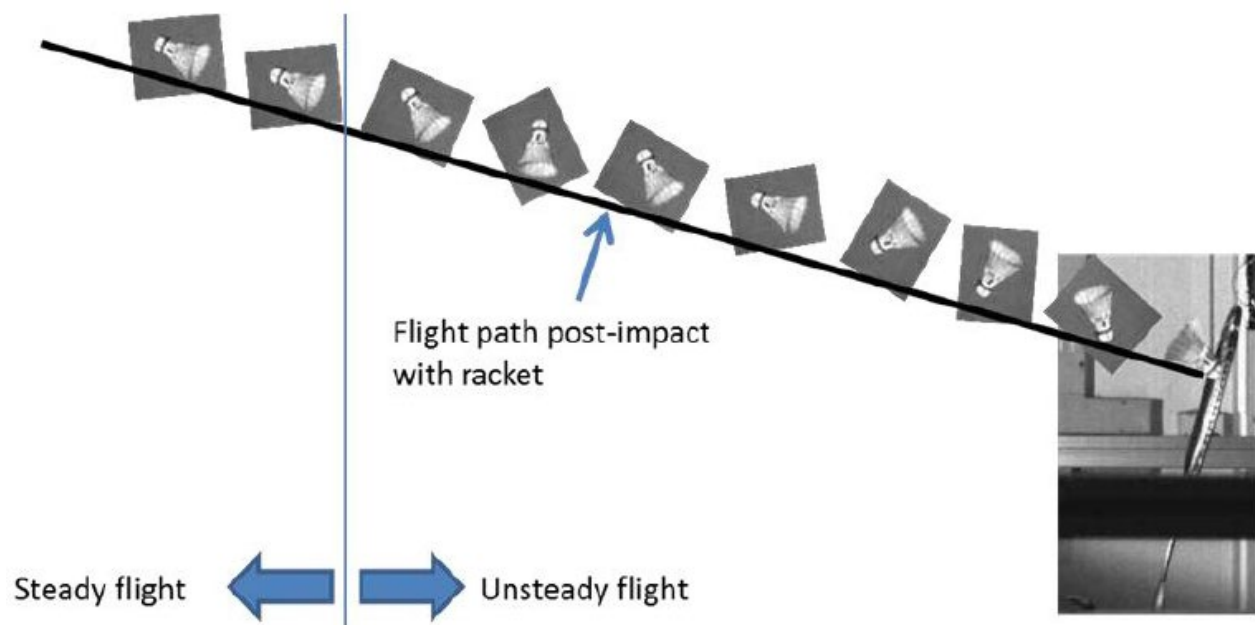


Figure 14: Transition of shuttlecock from unsteady state to steady state after impact with badminton [4].

Cao et al. [5] experimented with a wind tunnel which shows there is a time delay of 0.8sec at a flow speed of 20.3 m/s to achieve steady-state spin from the time when the shuttle leaves the racket. This braces the proposal that the spin of a shuttle is not instant.

The shuttlecock is designed in such a way that it spins clockwise direction along its longitudinal axis when viewed from the opposite end because of its pitching moment.

A group of Japanese researcher experimented on affect Axial rotation on drag coefficient, contrary to our belief there was no effect of rotation on the in-flight drag coefficient below Re no. 210000. Above which there was an increase in drag coefficient because of skirt expansion at high axial rotation because of high centrifugal push. Which is unlikely to happen in actual conditions as shuttlecock will never achieve this speed.

2.3.3 Summary

- 1.Flow visualization shows that the shuttle behaves like a bluff body and greater part of the drag is a base drag.
- 2.Experimentation shows that the coefficient of drag decreases as gap size reduces as compare to normal shuttlecock with gaps. Flow visualization showed that the jets of air passes through the hole and reduces the air pressure in the wake on the inner surface of the skirt. Which increases a pressure difference thereby increasing the drag coefficient.
- 3.Feather shuttlecock has much stronger axial jets and fluid near feathers acquire large tangential velocity which leads to streamwise vortices while in case of synthetic shuttlecock holes over skirt helps the fluid to move outside at the upper end of the skirt due to which its tangential velocity is significantly smaller.
- 4.Gaps on the lower portion of the skirt increases drag force over a gapless conical skirt. There is a critical gap size, below which drag increases as the gap widens and beyond which, as gaps increase blunt-body effect decreases, drag force reduces.
- 5.Axial rotation on drag coefficient, contrary to our belief there was no effect of rotation on the in-flight drag coefficient.

3. Aerodynamics of Shuttlecock

Eleven models of Shuttlecocks have been used for the computational study: one is reference shuttlecock(Model X), 4 of them are with axial and radial pressing, 2 with radial pressing only and 4 of them are with Axial pressing only, description of them is given in figure(16). The categorization of models is shown in the flow chart in figure(15). Further, Each Model(except model with axial pressing only, as there is no scope of a different pressing length overskirt) has 6 different models according to pressing length (i.e from 10mm to 60mm in the interlude of 10mm) over the skirt of the shuttlecock as shown in Fig(17) and labelled as Profile 1 - 6. The gapless model is of dimensions as discussed by Verma[2], CSH Lin[4], Cooke[1] in their work, with 1mm thickness as shown in fig 16(a). While in other models Diameter is increased by 2mm from 6mm to 67mm considering the synthetic shuttlecocks available in the market. Models consist of sixteen panels as of the feather shuttlecocks which consists of 16 trimmed feathers. Other dimensions of models are specified in figures 14.

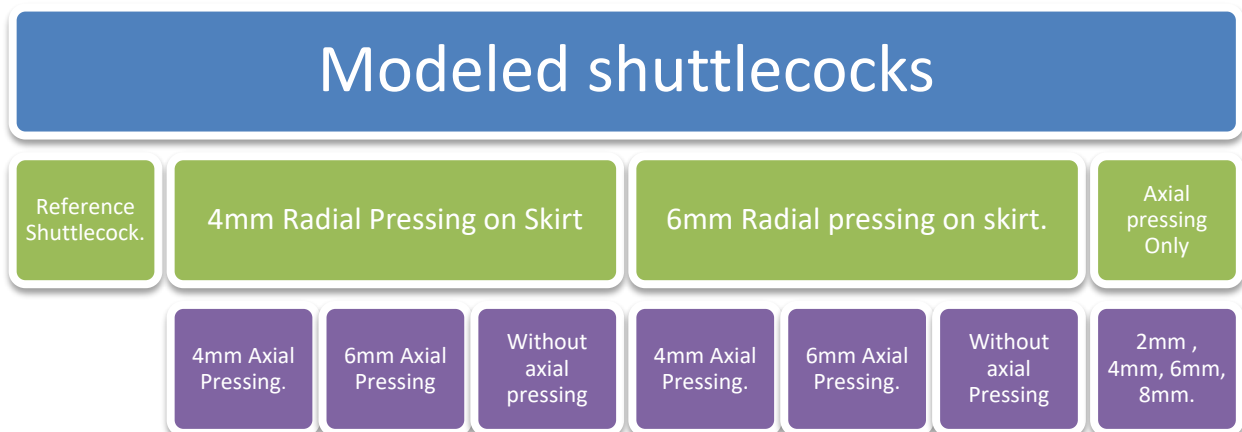


Figure 15: Classification of shuttlecocks.

A solid skirt shuttlecock is modelled with gapless cone, behind a cork of hemispherical dome shape which is evaluated using computational fluid dynamics (CFD). Its computational result was then validated with the computational results of verma[2] and computational and experimental results of CSH Lin[4]. which set out as the baseline reference and validate the result from previous work. Cones with different pressing were then compared with the gapless cone. The gapless model is expected to provide information on the role of pressing in the flow past a shuttlecock.

3.1 Model Geometry and ANSYS Fluent Method

A reference shuttlecock is modelled which is having a conical skirt thickness of 0.3mm, a skirt diameter of 65mm, and a length of 60mm. The skirt is attached to the cork which is made of the hemispherical and cylindrical parts of 13.20mm Radius and 11.80mm respectively. These were the dimensions that were referred from CSH Lin[5], Verma et al [2], and used in cooke[1] as shown in fig. 14(a). While in other models Diameter is increased by 2mm to 67mm Considering the synthetic shuttlecocks available in the market. Other dimensions of models are specified in figures (14).

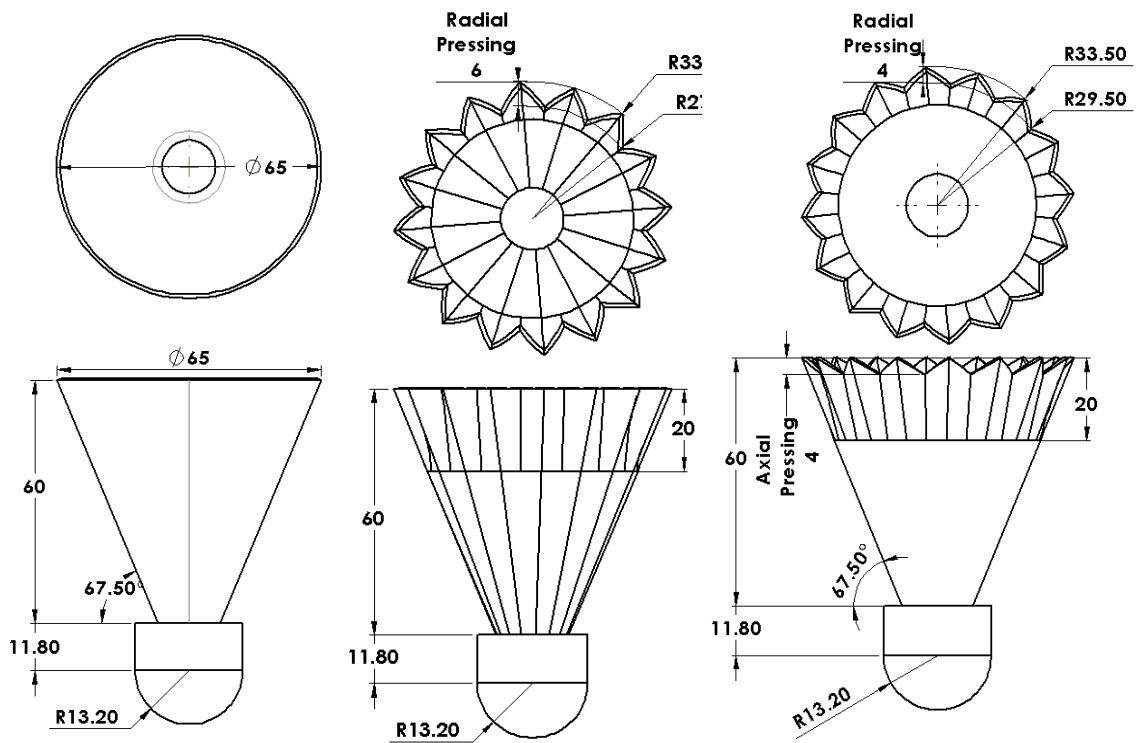


Fig. 16(a)

Fig. 16(b)

Fig. 16(c)

Figure 16: Different types of shuttlecocks, fig.14(a): gapless(Model X) shuttlecock without Axial and Radial Pressing used as reference, fig 14(b): Shuttle with 6mm Radial pressing and without Axial Pressing with 20mm of pressing length, fig 14(C): 4mm radial pressing 4mm axial pressing with 20mm length of pressing over skirt. All Dimensions are in mm.

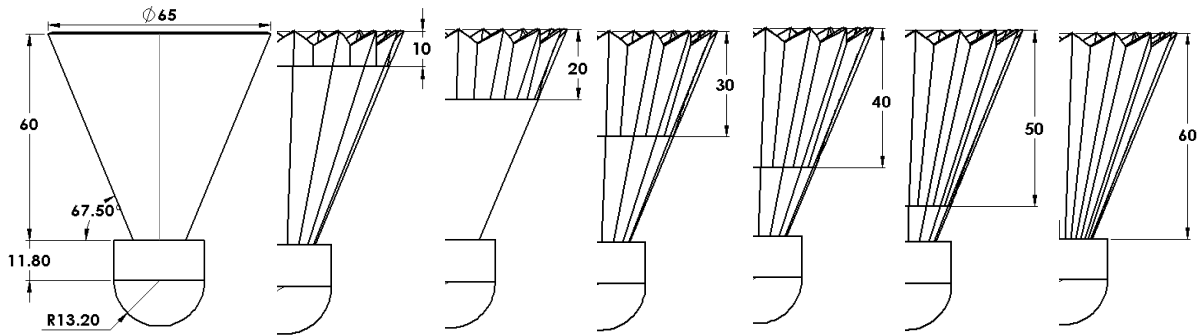


Figure 17: Different type of pressing length used in the models. Model X has no pressing while other models show pressing from 10mm to 60mm in an interval of 10mm and labelled as Profile 1-6. All dimensions are in mm.

- Skirt Surface area and frontal surface area of various shuttlecocks are given table 3.

Table 3: Skirt Surface area and frontal area of shuttlecocks.

The surface area of the shuttlecock skirt						
Shuttle Name	4R4A	6R4A	4R6A	6R6A	4RNN	6RNN
Pressing length						
1	0.811616	0.82088	0.790288	0.798552	0.855936	0.798537
2	0.812376	0.825504	0.788992	0.798752	0.899167	0.88176
3	0.812688	0.835056	0.799936	0.804016	0.906288	0.90235
4	0.814672	0.872496	0.7888	0.81096	0.878112	0.81096
5	0.81732	0.877195	0.789168	0.819424	0.88912	0.819424
6	0.821664	0.880896	0.79016	0.843216	0.941424	0.843216
Frontal Area	3137.61	2928.7	3139	2930.03	3104.19	2948.7

Table 3: Skirt Surface area and frontal area of shuttlecocks.

The surface area of the shuttlecock skirt					
Shuttle Name	NN2A	NN4A	NN6A	NN8A	Reference (Model X)
Skirt Area	0.848512	0.826288	0.793232	0.786224	8191.07
Frontal Area	3439.5	3370.8	3271	3271.4	3315.2

3.2 Nomenclature of shuttle name :

For ease of understanding the shuttlecock Models, Nomenclature is done for shuttlecock, description of 3 cases are shown in table1, table2 & table3. Not applicable indicate that this shuttlecock doesn't have that design feature.

1. 6RNN2

6	R	N	N	2
6mm	Radial Pressing	N.A.	N.A. (No Axial Pressing)	2cm~20mm Skirt pressing length.

Table 4: Example of Nomenclature of shuttlecock, having only Radial pressing of 6mm. As shown in Fig.16(b).

2. 4R4A2

4	R	4	A	2
4mm	Radial Pressing	4mm	Axial Pressing	2cm~20mm Skirt pressing length.

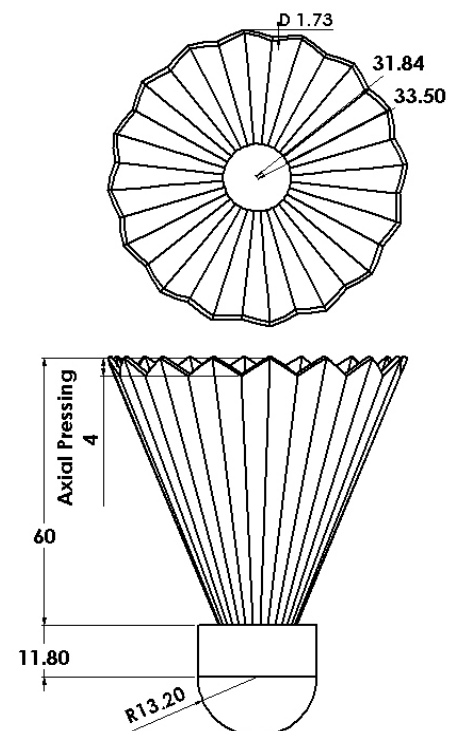
Table 5: Example of Nomenclature of shuttlecock, having 4mm radial & 4mm axial pressing over 20mm of skirt length. as shown in Fig.16(c).

3. NN4AN

N	N	4	A	N
Not applicable	Not applicable	4mm	Axial Pressing	Not applicable

Table 6: Example of Nomenclature of shuttlecock, having only Axial pressing of 4mm. As shown in Fig.18

Figure 18: Show Shuttlecock NN4A, Which is having 4mm Axial pressing only, D Shows radial pressing due to Axial pressing.



3.3 Mesh and Boundary conditions

. The mesh domain used in the computation is categorized into three zones using a sphere of influence Coarse: away from the shuttlecock, Medium, Fine: in the vicinity of a shuttlecock. Fig. (19) Shows Fine mesh case used for the computation of the 6R4A2 shuttlecock. It consists of 4.03 million unstructured elements with Blank nodes. A cylindrical flow field enclosure of 250mm Radius is formed around the shuttlecock model, with shuttlecock cork stagnation point at 165mm downstream to the inlet and the outlet at 650 mm downstream

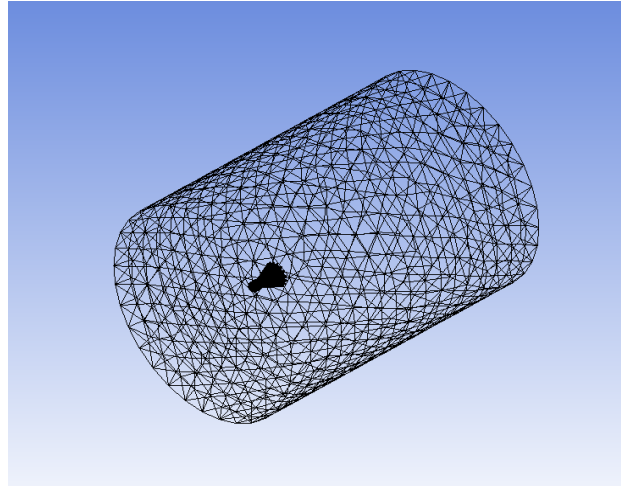
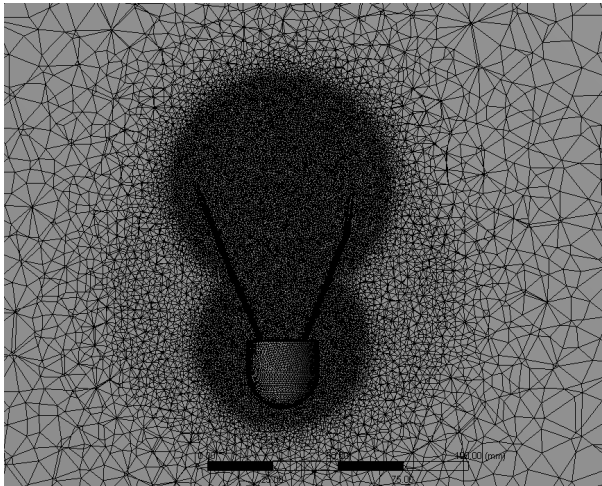


Figure 19: Mesh around shuttlecock.

Figure20: Shuttle within cylindrical fluid domain.

from the top of the shuttlecock skirt. In Ansys Fluent, the inlet of flow domain was selected as velocity inlet with its velocity 50m/s for every shuttlecock, while the outlet is set to pressure outlet with a 0 static pressure. The wall of the enclosure was set to symmetry which acts as a free slip wall, and the shuttlecock wall was set to the No-slip wall. Fig. (20) show a profile model within the cylindrical fluid domain.

3.4 Solution method

The computation is done in a fixed reference frame attached to the shuttlecock. Initially, a Realizable k-epsilon model was considered for computation but later Turbulent SST K-Omega is considered. Both of them are a 2-equation model but SST K-Omega is more precise in the vicinity of-wall boundary layer and its results found to agree with the previous experimental and computational resu

Its. A simple algorithm is used for pressure and velocity coupling. The effort is completely computational, to strengthen the validity of CFD simulation, computation is carried out for

gapless shuttlecock whose results are compared with the previous experimental and computational work. In this study, Fluid is considered to be incompressible and the shuttlecock is considered to be non-deformable, which occurs in actual flow condition due to fluid forces, the shuttlecock is having 0degree of the angle of attack and the spin of shuttlecock is also not considered.

The equation is utilized for the calculation of the coefficient of drag, which is reported quantity in the analysis

$$C_d = \frac{F_D}{\frac{1}{2}\rho A_D v^2}$$

Where C_d represents the drag coefficient, F_D represent the drag force, ρ represents the density of air, A_D represents the frontal area normal to the direction of travel and v represents the relative velocity of travel of the shuttlecock concerning air.

3.5 Validation

Flow past the different models is evaluated at a velocity of 50m/s. The numerical data obtained was validated by comparing the coefficient of Pressure of Model X(gapless shuttlecock) with the coefficient of Pressure of Verma [2] as shown in figure(6), and Computational and experimental result of CSH Lin[4]. Coefficient of pressure trend is found to be same in all the three cases.

The drag coefficient for gapless shuttlecock: Model X is 0.4941, and the drag coefficient obtained by C.S.H Lin[4] from the experiment is 0.491 and by the computational method is 0.514. The difference in the drag coefficient drawn from the experimental result is 0.63% and from the computational result is 4.04% which can be considered as in good agreement. This same computational method and boundary condition are applied to the other shuttlecock models for evaluation of drag coefficient and flow fields.

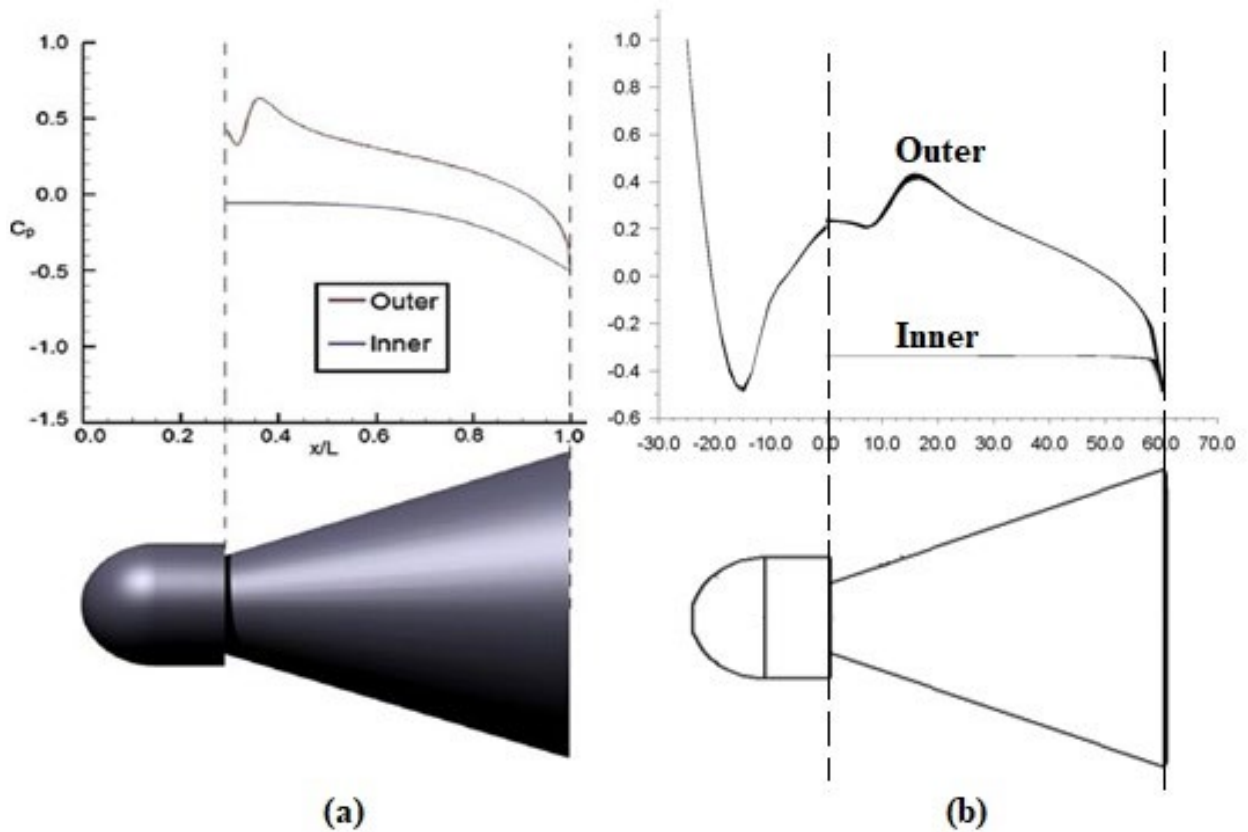


Figure 21: Shows the Coefficient of pressure result x axis shows length of the shuttlecock in and y axis Shows Pressure coefficient. Fig.21(a) Result from Verma [3], On x axis length is given in X/L, Fig. 21(b): Result for model X(Reference Model), Length is given in mm, upper curve show pressure coefficient on outer surface and lower curve shows pressure coefficient on inner surface.

3.6 Grid- Independent Test

Analysis of grid independence was accomplished by comparing the numerical drag coefficient for the applied mesh and for a refined version of the applied mesh on one shuttlecock of each type of pressing. Simulation is given the insight that a grid of between 1 to 1.6 million volumes is adequate for grid independence. Comparison between the applied mesh and the refined mesh version shows that the drag coefficient lies within +/- 3% which is sufficient for grid independence. The numerical results of the grid independency study are shown in Table 10. All the shuttlecocks which are considered for comparison were having a flow velocity of 50m/s. The drag coefficient of different models is shown in figure 23.

Table 7: Difference in Drag coefficient from the course and Fine mesh. Elements are in millions.

Profile	Applied Mesh		Refined Mesh		Difference
	Elements	Drag coefficient	Elements	Drag Coeff	
4R4A2	0.3729	0.4215	1.01	0.428	1.54%
6R4A2	0.374	0.38266	4.062	0.38557	0.760%
6R6A2	0.993	0.3991	1.51	0.3967	0.60%
4RNN2	0.361	0.4136	1.53	0.40421	2.73%
6RNN3	0.451	0.36	2.89	0.355	1.38%
Reference	0.369	0.4941	1.01	0.483	2.24%

4. Result and Discussion

4.1 Flow Over a Perfect Gapless Conical Skirt

The defined numerical method is used for calculating the drag coefficient of Profile X at flow speeds of 50m/s. Drag coefficient from the higher speed 50 m/s provides a comparison with previous work, as in [3]. This also validates model used in our study.

The flow behaviour around the gapless shuttlecock(Model X) is also studied. Velocity vector around the shuttlecock at the velocity of 50m/s is shown in figure(22). The most remarkable highlight of the vector plot is a couple of counter-rotating vortices in the wake region next to the skirt, extending in the upstream direction into the low-pressure region of the cone inner surface. The presence of this pair of vortices produces an inward curling effect on the flow around the core region in the near field wake. This curling effect extends to a low magnitude reverse flow which can go less than 2 m/s that pushes in towards the low-pressure inner surface of the cone. Cooke [2] concluded the same result for shuttlecock in her experimental.

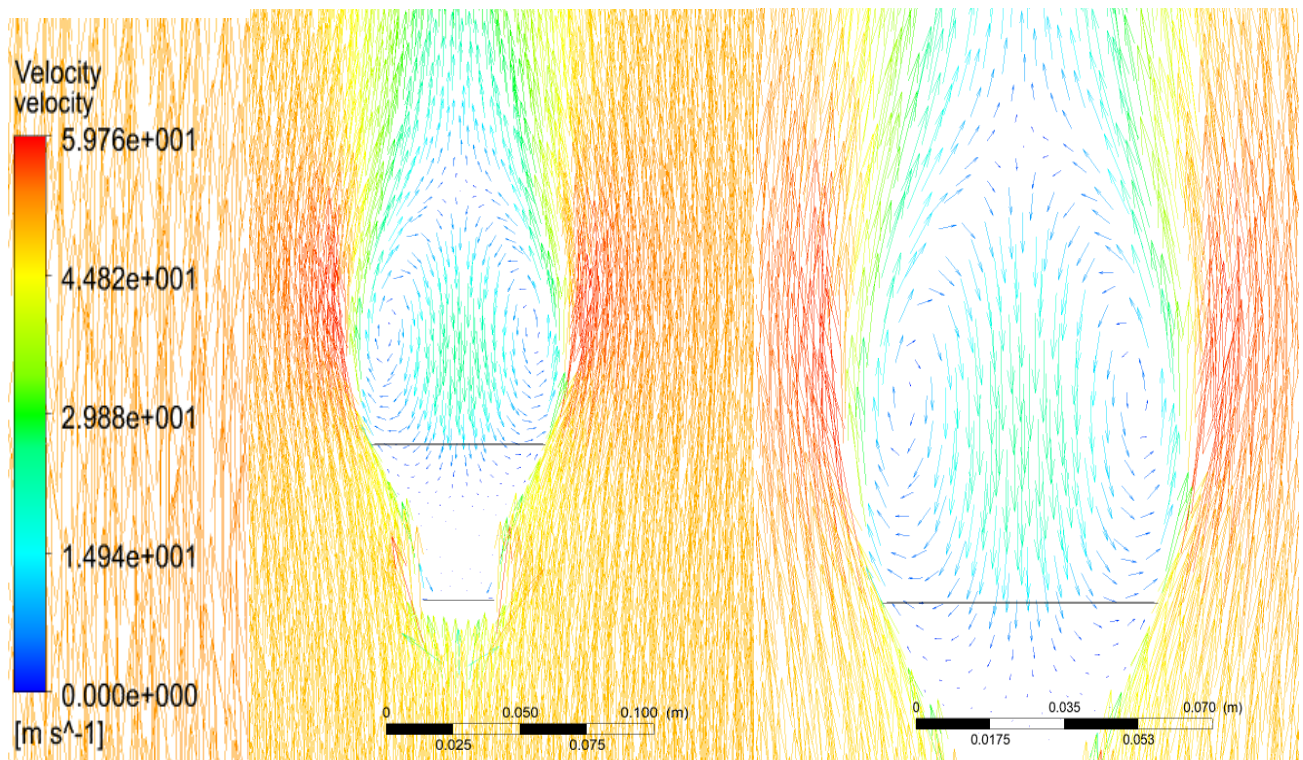


Figure 22: Velocity vector around a gapless shuttlecock.

4.1 Drag Coefficient

- Fig.23 shows the variation of the drag coefficient in the different model at a velocity of 50m/s. The result from the reference model(Model X), as well as form other models, are presented.

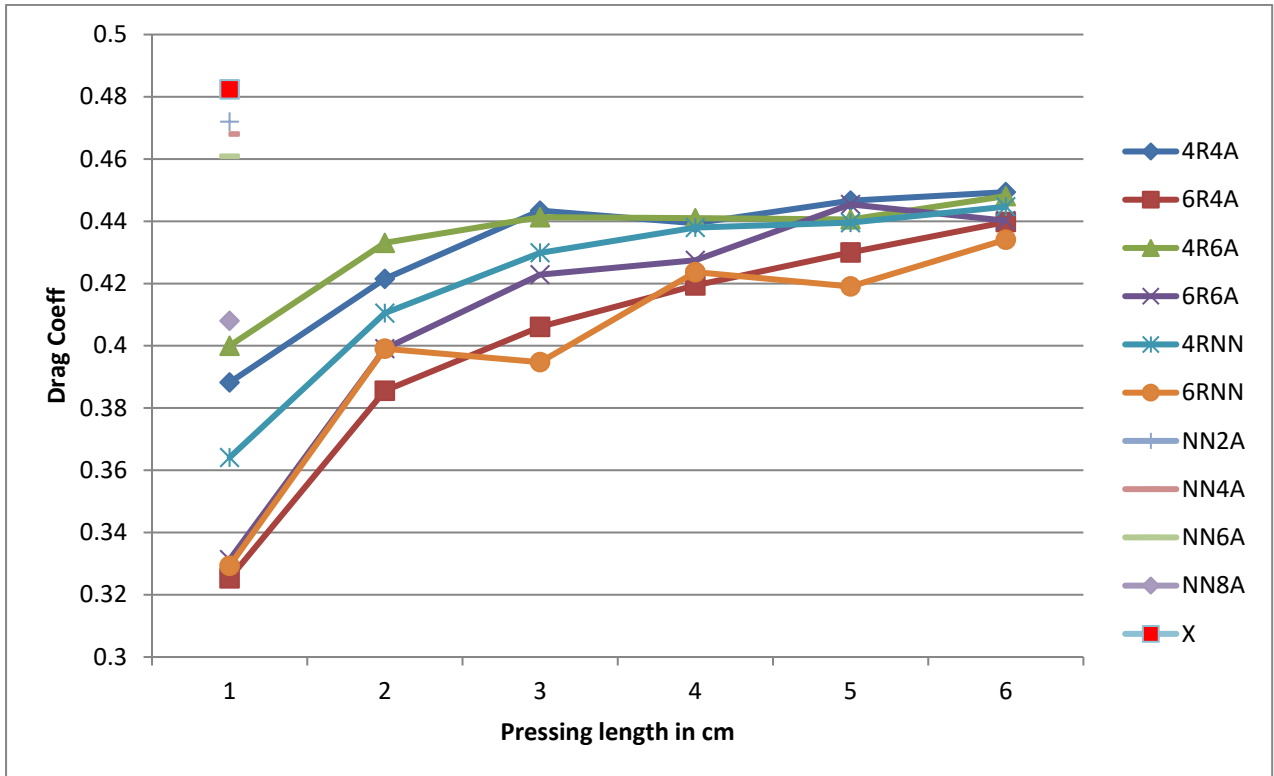


Figure 23: Variation of drag coefficient of various models with different pressing length.

- The drag coefficient for 4R4A1 and 4R4A6 is found to be in the range of 0.3882 to 0.4494 at 50m/s which is a change of 15.75%. The difference in drag of other models at 10mm and 60mm skirt pressing length is shown in Table 8.

Table 8: Difference in drag on 10mm ad 60mm skirt pressing length.

Shuttlecock	4R4A	6R4A	4R6A	6R6A	4RNN	6RNN
The difference in Drag. (%)	15.751	35.194	20.6	32.86	22.131	31.82

- The difference in a drag coefficient of model 4R4A1 and 6R4A1 is 19.33%. The difference in drag coefficient decreases when pressing length increases over the skirt surface and difference remain 2.136% for 4R4A6 and 6R4A6.

- In the case of 6R6A, 6R4A, 6RNN the drag coefficient Increases rapidly from pressing length 10mm to 20mm. In 20 to 60mm pressing length drag coefficient increase at a constant rate which is quite less than the rate in 10mm to 20mm.
- In case of 4R4A, 4R6A, 4RNN the drag coefficient changes rapidly when pressing length changes from 10mm to 30mm, between 30mm to 60mm drag Coeff remains almost same and become independent of pressing length overskirt at a velocity of 50m/s.
- For all cases as the pressing length increases over the surface, drag coefficient also increases, this is because of the increase of surface area which increases the viscous drag, skirt surface area of the various model with different pressing length are shown in fig.24.

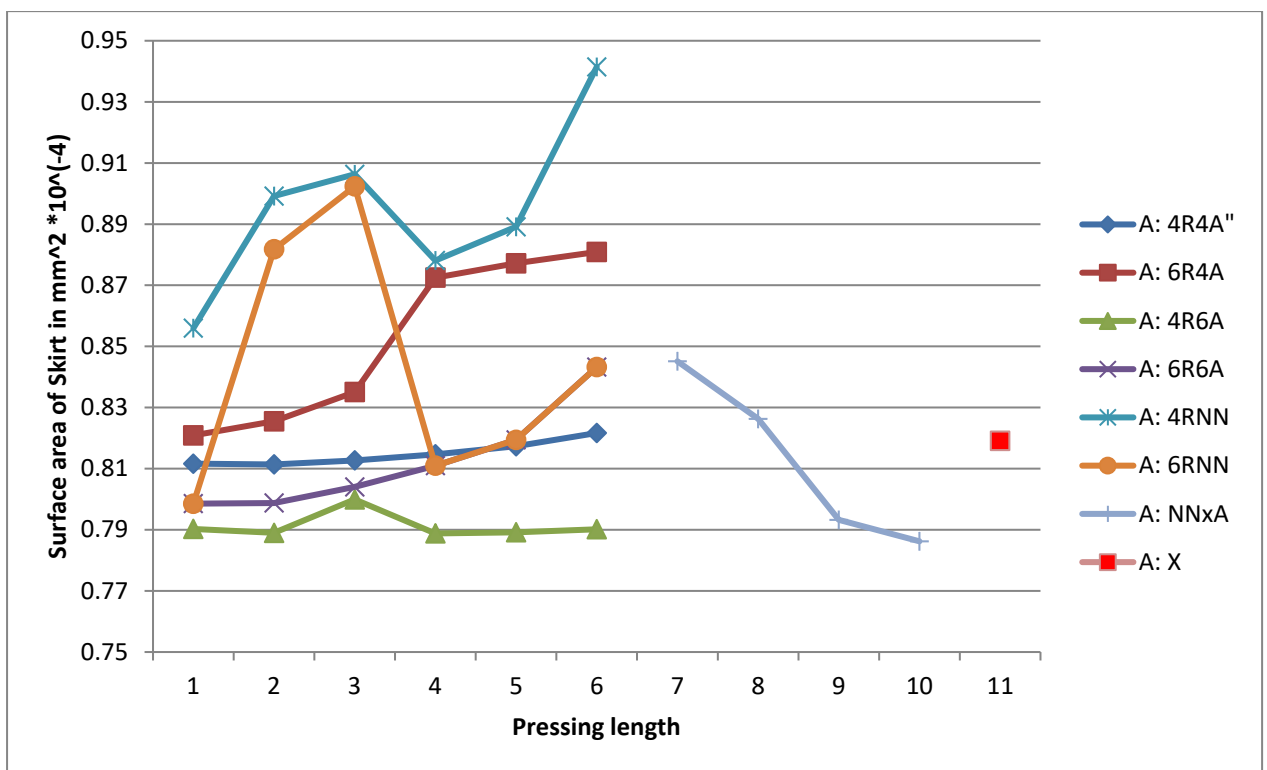


Figure 24: Variation of Skirt Surface area with Pressing length. On x-axis 1-6 represent the pressing length, while 7-10 represents Shuttlecock with an only axial pressing of 2,4,6,8mm respectively and 11 represent Model X. Area is in $mm^2 * 10^{-4}$.

- As radial pressing increases drag coefficient decreases because of a decrease in frontal area, this also shows the blunt-body property of shuttlecock, effect of frontal area on drag coefficient is shown in Fig 25.
- Interestingly, when radial pressing and axial pressing are combined the drag coefficient increases. 4R4A2 has a drag coefficient of 0.4215 while 4RNN2 have a drag

coefficient of 0.4105, this shows Drag coefficient increases when both Axial and Radial pressing is present in the model, Otherwise, any one of the pressings reduces the drag coefficient, a similar trend is seen in 6R4A2 and 6RNN2 where the drag coefficient is 0.367, 0.340 respectively.

- As axial pressing increases from 2mm to 8mm, the drag coefficient decreases 0.472 to 0.408 for NN2A and NN8A i.e 13.6% of the difference, this is because of decrease of the frontal area as well as a decrease in Skirt surface area as shown in fig.23 & fig.24 respectively.
- Drag coefficient variation follows the trend of the frontal area as shown in figure(25). But the change rate decreases as the pressing length overskirt increases.
- Model x has a maximum drag coefficient of 0.4825 as it has a maximum frontal area and moderate skirt surface area, which shows the dominant behaviour of frontal area on the drag coefficient.
- When Axial and Radial pressings are combined, the shuttlecock behaves differently. In a combined state as radial pressing increase drag Coefficient decreases for eg. Drag coefficient of 4R4A ad 6R4A is 0.388 & 0.325 respectively, contrary to this when axial pressing increases drag coefficient increases considering another factor as constant for eg. Drag coefficient of 6R4A & 6R6A are 0.406, 0.423 respectively. This trend is followed at all the pressing lengths as shown in fig.23.

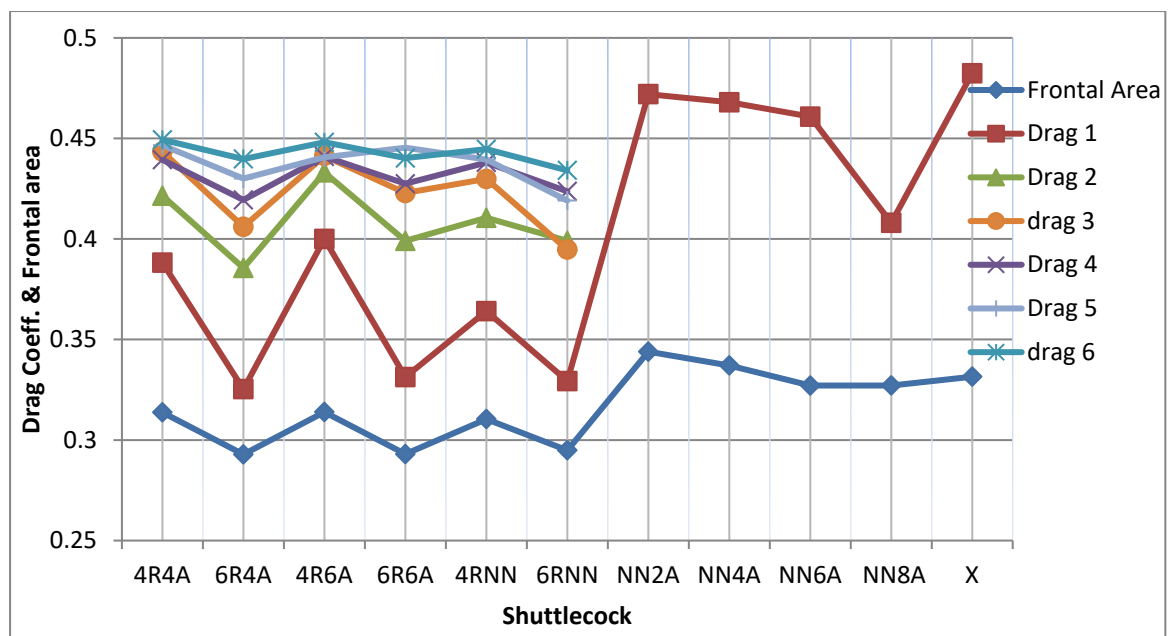
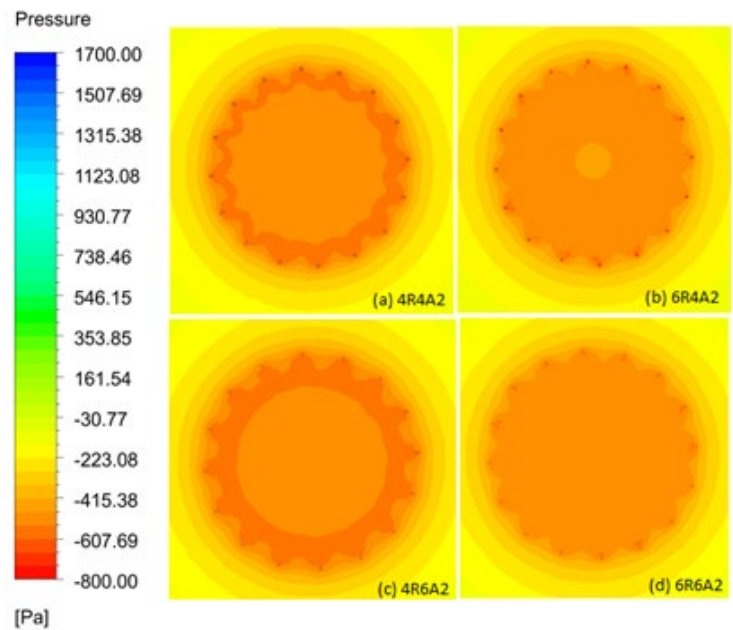


Figure 25: Drag coefficient & Frontal area Vs. Shuttlecock. Drag 1 to Drag 6 Represent pressing length of 10mm to 60mm overskirt.

- This increase in Drag coefficient in the combined state is because of flow behaviour around the top portion of the skirt which creates a pressure difference on the inner and outer side of the shuttlecock. Figure (26) shows the pressure contours on the top portion of shuttlecocks which are having 20mm length of skirt pressing.



- The pressure variation along the radial distance is shown in figure(27), pressure trend completely follows the trend of drag coefficient of their respective shuttlecock. For instance, the drag coefficient of 4R6A2 is maximum out of all other shuttlecocks of 20mm pressing as shown in Figure(23), this same shuttle has minimum pressure in the wake zone. Which increases the pressure difference around the shuttlecock and hence the drag coefficient.

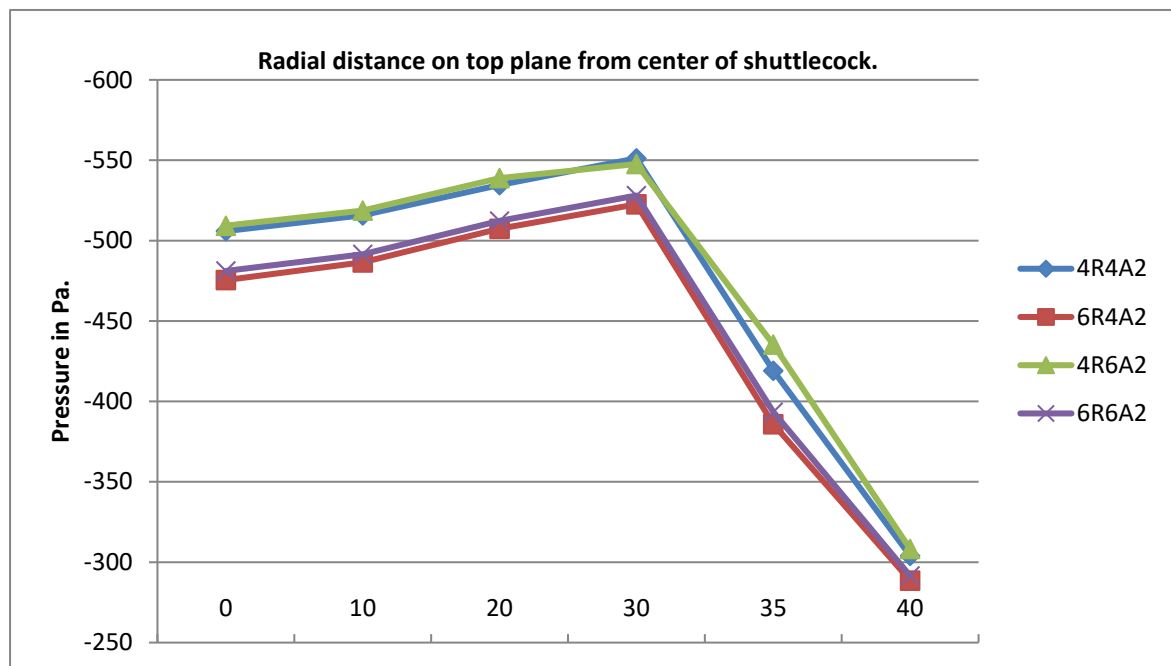


Figure 27: Pressure vs. radial distance from the centre of the shuttlecock on the top portion of the shuttlecock.

- The results are different from those obtained from turbulent SST K-Omega model and Realizable K-Epsilon model, the difference in result for model 6R4A2 is 8.27%, the difference in result for few cases is shown in Figure(28). The result obtained from SST k-Omega is closer to the results of previous studies. There is a constant difference between results obtained from K-omega model and K-Epsilon model.

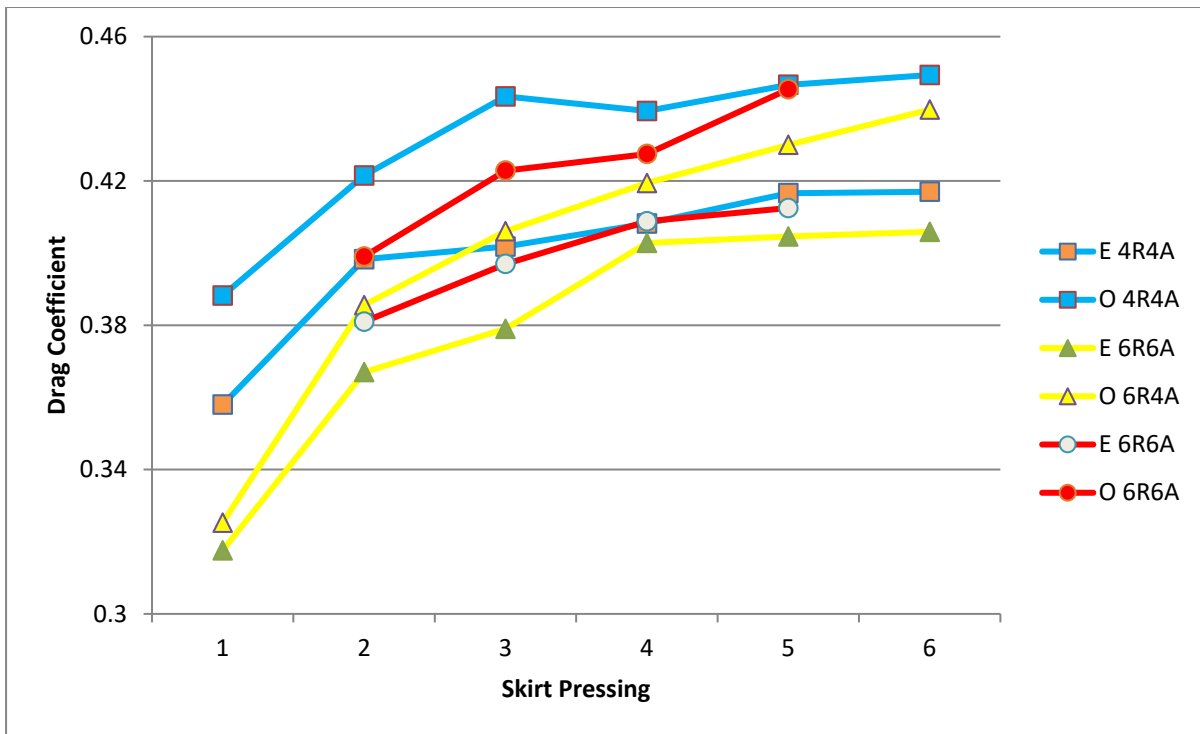


Figure 28: Drag Coefficient Vs. Skirt pressing with Different Models, E represents the K-Epsilon model, whereas O represents K-Omega model.

5. Conclusion

Through the 3D CFD simulation conducted using Ansys Fluent, The impact of different pressing over shuttlecock with different pressing length was analysed. The principal conclusions of the analysis are as follows:

- Radial pressing on shuttlecock decreases Drag coefficient, as frontal area decreases.
- Axial Pressing decreases Drag coefficient at a slow rate initially. Later on, behaves as radial pressing and decreases drag coefficient rapidly as it also decreases the frontal area of shuttlecock reasonably.
- When Axial and Radial pressings are combined, the shuttlecock behaves differently. In a combined state drag coefficient increases when axial pressing is increased at the same radial pressing. Drag coefficient decreases when radial pressing is increased at a constant axial pressing,
- Drag coefficient increases as the pressing length overskirt increases, because of the increase in surface area which increases the viscous drag.
- For the Same axial and radial pressing variation in drag coefficient is prominent when pressing length changes from 10mm to 30mm and between 30mm to 60mm variation in drag is almost negligible.
- The frontal area has more effect on drag coefficient variation than that of the skirt surface area.

Future research.

No Data has been found on the spin variation along the path and how its axial speed variation affects the aerodynamics of shuttlecock in an unsteady state. Which will also give a further understanding of the purpose of providing pressing overskirt. No work has been done gyroscopic precision of shuttlecock. Furthermore, changing the other design parameter will give an insight into the shuttlecock behaviour. This will give a complete understanding of the aerodynamics of synthetic shuttlecock and will help in producing a shuttlecock with alike performance as of Feather shuttlecock.

REFERENCES

1. Cooke, A.J., *The aerodynamics and mechanics of shuttlecocks*, in *Department of Engineering* 1992, University of Cambridge: New hall, Cambridge.
2. Verma, A., Desai, A. and Mittal, S., 2013. Aerodynamics of badminton shuttlecocks. *Journal of fluids and structures*, 41, pp.89-98.
3. Kitta, S., H. Hasegawa, M. Murakami, and S. Obayashi, *Aerodynamic properties of a shuttlecock with spin at high Reynolds number*. *Procedia Engineering*, 2011
4. Lin, C.S.H., Chua, C.K. and Yeo, J.H., 2014. Aerodynamics of badminton shuttlecock: Characterization of flow around a conical skirt with gaps, behind a hemispherical dome. *Journal of Wind Engineering and Industrial Aerodynamics*, 127, pp.29-39.
5. Cao, X., J. Qiu, X. Zhang, and J. Shi, *Rotation Properties of Feather Shuttlecocks in Motion*. *Procedia Engineering*, 2014. **72**: p. 732-737.
6. Calvert, J.R., *The seperated flow behind axially symmetric bodies*, 1967, Cambridge University: Cambridge, UK.
7. Alam, F., Chowdhury, H., Theppadungporn, C. and Subic, A., 2010. Measurements of aerodynamic properties of badminton shuttlecocks. *Procedia Engineering*, 2(2), pp.2487-2492.
8. Hart, J., 2014. Simulation and understanding of the aerodynamic characteristics of a badminton shuttle. *Procedia engineering*, 72, pp.768-773.
9. Cooke, A., 2002. Computer simulation of shuttlecock trajectories. *Sports Engineering*, 5(2), pp.93-105.
10. A Study of Shuttlecock's Trajectory in Badminton. Available from: <https://www.ncbi.nlm.nih.gov/pmc/articles/PMC3761540/>
11. Shuttlecock design and development y Alison J. Cooke. *The Engineering of Sports*, Haake. Pg 91-95.
12. Cohen, C., Darbois-Texier, B., Dupeux, G., Brunel, E., Quéré, D. and Clanet, C., 2014. The aerodynamic wall. *Proceedings of the Royal Society A: Mathematical, Physical and Engineering Sciences*, 470(2161), p.20130497.
13. https://www.princeton.edu/~asmits/Bicycle_web/blunt.html